ORIGINAL ARTICLES

Intraoperative optical coherence tomography of the human thyroid: Feasibility for surgical assessment

SARAH J. ERICKSON-BHATT, KELLY J. MESA, MARINA MARJANOVIC, ERIC J. CHANEY, ADEEL AHMAD, PIN-CHIEH HUANG, Z. GEORGE LIU, KELLY CUNNINGHAM, and STEPHEN A. BOPPART

URBANA, ILLINOIS AND MADISON, WISCONSIN

Thyroid nodules assessed with ultrasound and fine-needle aspiration biopsy are diagnosed as "suspicious" or "indeterminate" in 15%–20% of the cases. Typically, total thyroidectomy is performed in such cases; however, only 25%–50% are found to be cancerous upon final histopathologic analysis. Here we demonstrate optical coherence tomography (OCT) imaging of the human thyroid as a potential intraoperative imaging tool for providing tissue assessment in real time during surgical procedures. Fresh excised tissue specimens from 28 patients undergoing thyroid surgery were imaged in the laboratory using a benchtop OCT system. Three-dimensional OCT images showed different microstructural features in normal, benign, and malignant thyroid tissues. A similar portable OCT system was then designed and constructed for use in the operating room, and intraoperative imaging of excised thyroid tissue from 6 patients was performed during the surgical procedure. The results demonstrate the potential of OCT to provide real-time imaging guidance during thyroid surgeries. (Translational Research 2018;195:13–24)

INTRODUCTION

Thyroid cancer is the most common cancer of the endocrine system, and the National Cancer Institute

From the Beckman Institute for Advanced Science and Technology, University of Illinois at Urbana-Champaign, Urbana, Illinois; Morgridge Institute for Research, University of Wisconsin, Madison, Wisconsin; Department of Electrical and Computer Engineering, University of Illinois at Urbana-Champaign, Urbana, Illinois; Department of Bioengineering, University of Illinois at Urbana-Champaign, Urbana, Illinois; Carle Foundation Hospital, Urbana, Illinois; Carle Illinois College of Medicine, University of Illinois at Urbana-Champaign, Urbana, Illinois.

predicted 56,870 new cases of thyroid cancer and 2010 deaths in the United States in 2017.[1] The thyroid gland consists of 2 connected lobes located at the front of the neck, which wrap around the trachea. The gland produces the hormones L-thyroxine (T4) and L-triiodothyronine (T3), which regulate metabolic physiological processes, cellular respiration, total energy expenditure, growth and maturation of tissues, and turnover of hormones, substrates, and vitamins. Parathyroid glands, located at the back of the thyroid, produce parathyroid hormone, which, along with calcitonin, is involved in regulating the amount of calcium in the blood and bones.[2]

After manual palpation of the neck as part of the physical examination, ultrasonography is often the first imaging modality employed to evaluate the presence of a thyroid nodule because it is readily accessible, inexpensive, noninvasive, and requires no radiation exposure. Ultrasound imaging is also effective at delineating intrathyroidal architecture, distinguishing cystic from solid lesions,

AT A GLANCE COMMENTARY

Erickson-Bhatt SJ, et al.

Background

About 15%–25% of thyroid nodule cases are found to be "cytologically indeterminate." Partial or total thyroidectomy is recommended in most indeterminate cases because of the possibility of carcinoma; however, only about 25%–50% of the cases are found to be cancerous by postsurgical histologic analysis.

Translational Significance

Optical coherence tomography has demonstrated the ability to distinguish normal, benign, and malignant thyroid tissue on ex vivo specimens. From benchtop to the operating room, this article demonstrates the feasibility and potential of optical coherence tomography as a tool for intraoperative surgical guidance during thyroid procedures, which can reduce patient morbidity.

determining if a nodule is solitary or part of a multinodular gland, and accurately locating and measuring the dimensions of a nodule. However, ultrasonography is dependent on an ultrasonographer for the quality of images, regions of the neck covered, and interpretation. Other less common methods include radionuclide imaging, positron emission tomography, single-photon emission computed tomography, x-ray computed tomography, and magnetic resonance imaging, but these clinical imaging modalities are usually insufficient to provide accurate diagnosis of malignant nodules. Therefore, fine-needle aspiration biopsy (FNAB) is currently used as the gold standard for deciding whether to proceed with surgical treatment of thyroid nodules. FNAB results in 4 possible diagnoses: (1) benign nodule (occurs in ~70% of the cases; the recommended procedure is usually to follow the nodule without surgery); (2) malignant nodule (occurs in 4% of the cases; the recommended procedure is usually partial or total thyroidectomy); (3) suspicious nodule (occurs in 15%–25% of the cases; the surgeon determines case-by-case how to proceed—typically total thyroidectomy or possibly lobectomy with frozen section analysis to determine malignancy); (4) nondiagnostic (which occurs in 5%–10% of the cases when insufficient cytologic material is present to make a diagnosis; the typical procedure is to repeat the FNAB or proceed with surgery).[2-4]

About 15%–25% of thyroid nodule cases are found to be "cytologically indeterminate" and termed as follicular neoplasm, suspicious for carcinoma, or atypical.[5-7]

This finding may be due to various benign cellular or nuclear changes, which can be indistinguishable from papillary carcinoma, which can be metastatic. Additionally, features such as capsular penetration and vascular structures indicative of follicular carcinoma cannot be discerned in aspiration cytology because of disruption of the tissue architecture. The American Thyroid Association and the European Thyroid Association have recommended partial or total thyroidectomy in most indeterminate cases because of the possibility of carcinoma; however, only about 25%–50% of the cases are found to be cancerous by postsurgical histologic analysis. Hemithyroidectomy is preferred when possible because of lower morbidity,[8] and many patients will not require exogenous levothyroxine if half of the thyroid is functional.[6]

Optical coherence tomography (OCT) is the optical analogue to ultrasound imaging, but uses broadband near-infrared light to produce much higher-resolution images with the tradeoff of reduced imaging depth penetration[9] (1). OCT has been widely used for clinical ophthalmic imaging[10] (2) and has demonstrated clinical translation in other areas as well, including gastroenterology,[11,12] dermatology,[13,14] cardiology,[15,16] and primary care.[17] OCT has also been used for cancer imaging and demonstrated the capability of imaging breast cancer intraoperatively[18-20] and in vivo within the surgical cavity[21] for real-time surgical guidance. OCT has demonstrated the ability to distinguish normal, benign, and malignant thyroid tissue on ex vivo specimens,[22,23] as well as to identify thyroid and parathyroid glands on ex vivo specimens and intraoperatively.[24,25] However, none of these studies have demonstrated the ability to image in vivo. From benchtop to the operating room, this article demonstrates the feasibility and the potential of OCT as a tool for intraoperative surgical guidance during thyroid procedures.

MATERIALS AND METHODS

Benchtop OCT system. The benchtop OCT system (Fig 1) consisted of a superluminescent diode source with 1310-nm center wavelength and 170-nm bandwidth. A 50/50 fiber coupler was used to split the beam between the reference and sample arms. The axial and transverse resolutions of the system were 6 and 16 µm, respectively. The optical power at the sample was less than 10 mW. Reflected light was detected using a spectrometer in this spectral-domain OCT configuration. The tissue was placed in a dish and noncontact imaging was performed in the *x-y* lateral directions (using 2 computer-controlled galvanometer-scanning mirrors), as well as in the axial (*z*) direction to generate 3-dimensional (3D) image data, which were immediately displayed on the computer monitor.
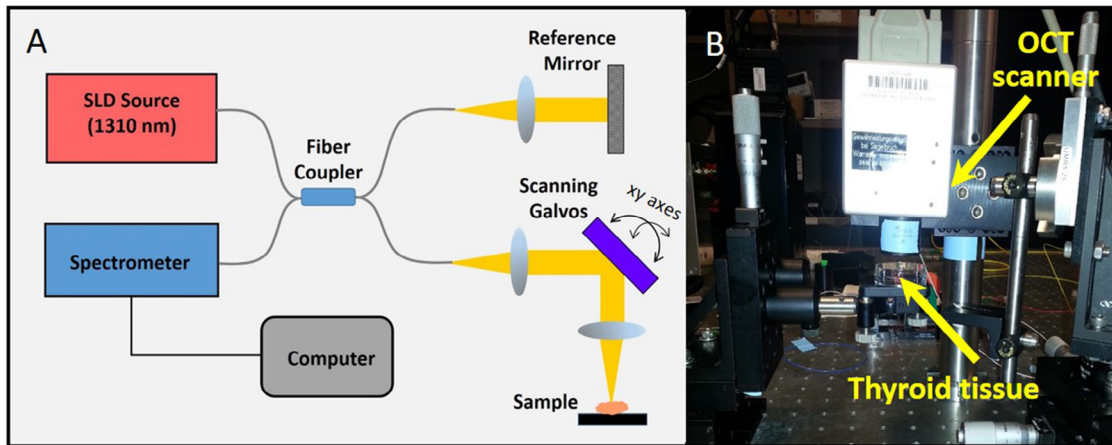
Fig 1. (A) Schematic of the benchtop OCT system. (B) Photograph of the system showing the position of the tissue during imaging. OCT, optical coherence tomography; SLD, superluminescent diode.

Ex vivo imaging using the benchtop OCT system. The ex vivo human tissue studies were approved by the Institutional Review Boards at the University of Illinois at Urbana-Champaign and the Carle Foundation Hospital, Urbana, Illinois, and written informed consent was provided by all subjects. More than 100 tissue samples from 28 patients undergoing partial, total, or completion thyroidectomy were imaged. During histologic processing after surgery, small samples (~1.0–1.5 cm) of thyroid tissue were selected by the pathologist assistant from the visually normal and abnormal regions of the same thyroid and were placed in saline on ice. The samples were transported to the laboratory to be imaged using the benchtop OCT system within 12 hours. After OCT imaging, the tissues were inked at the imaging location and processed and stained in-house by the researchers with hematoxylin and eosin for correlation

with OCT images. The histology slides were viewed independently by a board-certified pathologist at the Carle Foundation Hospital to assess whether the slice corresponding to the OCT image contained malignant, benign, or normal thyroid tissue, as indicated on the final pathology report.

Intraoperative imaging using a portable OCT system. A portable custom-designed spectral-domain OCT system was designed and constructed to be easily maneuvered into the operating room and positioned close to the surgical field for real-time imaging during surgical procedures. The intraoperative OCT system (Fig 2) also used a superluminescent diode source (Praevium Research, Inc; 1330 nm center wavelength, 105 nm bandwidth) and a 50/50 fiber coupler to split light between the sample arm (the handheld surgical probe) and the reference arm. The reflected light was detected by a
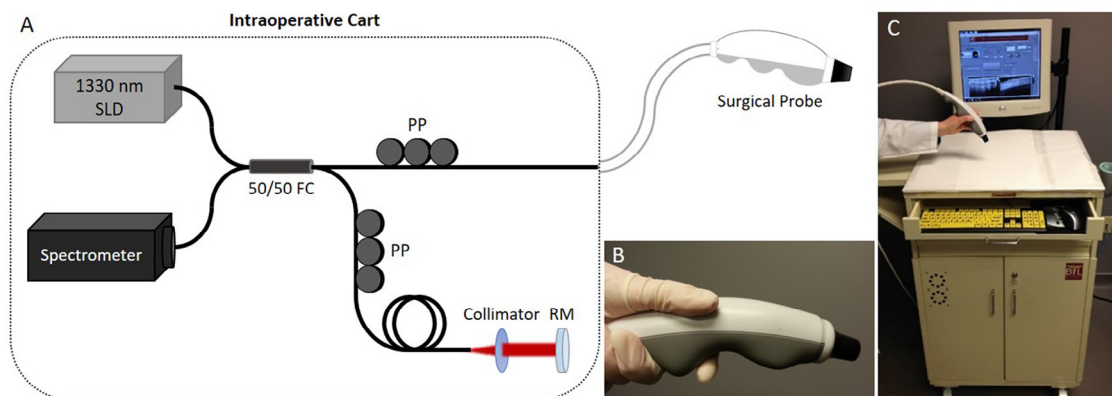

Fig 2. The intraoperative OCT imaging system. (A) Schematic showing the intraoperative OCT system components. (B) The sample arm is a handheld surgical probe used to image excised specimens. (C) The OCT system is integrated in a portable cart for easy transportation into the operating room and positioning near the sterile surgical field. SLD, superluminescent diode; FC, fiber optic coupler; PP, fiber polarization paddle controller; RM, reference mirror; OCT, optical coherence tomography.

spectrometer and the 2-dimensional OCT images (B-scans) were displayed in real time on the computer screen with both axial and transverse resolutions of approximately 9 μm, an image scan width of 8.8 mm, and a frame rate of 11.5 frames/s. The laser power on the tissue was less than 10 mW.

Procedure for intraoperative imaging of thyroid specimens. The intraoperative study was also approved by the Institutional Review Boards at the University of Illinois at Urbana-Champaign and the Carle Foundation Hospital, and written informed consent was provided by all subjects. The portable OCT system was brought into the operating room, outside of the sterile field, during the surgeries. The probe was covered with 2 sterile and optically transparent plastic sheaths and placed in contact with the fresh tissue specimens during imaging. In each case, the surgeon resected the thyroid, palpated the specimen, and subsequently made an incision along the longest axis of the thyroid as shown in Fig 3, with the future histologic section plane depicted in blue. The tissue was then immediately given to the researchers for imaging the samples in a sweeping pattern. Real-time OCT frames were displayed on the monitor and saved for later post-processing. The real-time images were viewed only by the researchers in the present study and were not used by the surgeon for diagnostic or surgical guidance purposes. Typically, 1–3 areas were imaged for each tissue sample, and the imaging time for each specimen was less than 1 minute. Because of the standard tissue histologic sectioning protocols at the Carle Foundation Hospital, OCT imaging was performed in planes orthogonal to the histologic sectioning planes, as depicted in Fig 3. Typically, the OCT imaged area was identified by the application of surgical ink. However, during the intraoperative imaging portion of the present study, this technique was not allowed. Thus, after OCT imaging, the sample was placed in preserving solution (formalin) and sent for histologic processing. The pathologist received the entire specimens with the surgical incisions made in the operating room for OCT imaging. The pathologist subsequently incised the tissue along the same direction as the incision in the operating room and generated histologic slides of these imaged areas. The remainder of each tissue specimen was grossly dissected and submitted for histologic processing and evaluation, as per standard of care. Histology slides from the OCT imaged areas were digitized with a slide scanner (NanoZoomer 2.0 RS, Hamamatsu C10730, Hamamatsu Photonics, K.K.), and correlations were made between the OCT images in the corresponding histologic sections.

RESULTS

Ex vivo benchtop 3D OCT imaging of normal, benign, and malignant human thyroid tissues. OCT images from the benchtop system were collected from 28 patients undergoing partial, total, and completion thyroidectomies. Table I shows the distribution of patients by gender and age (note that only 2 patients were male, which was consistent with thyroid diseases being more prevalent in females). The table lists the preoperative diagnosis (determined by FNAB), the surgical procedure, and the final postoperative diagnosis (from histopathologic analysis) for each patient. Out of 28 patients, 14 had a preoperative diagnosis of a "suspicious" or indeterminate nodule. Of these 14 patients, 13 underwent total thyroidectomy (~93%), and only 5 of the 13 (~38%) were found to be malignant upon final histologic analysis. This finding is consistent with the statistics from the American and European Thyroid Associations.[6]

Representative examples of OCT images of normal and benign thyroid tissues are shown in Fig 4. The apparent differences in size or area of tissue between
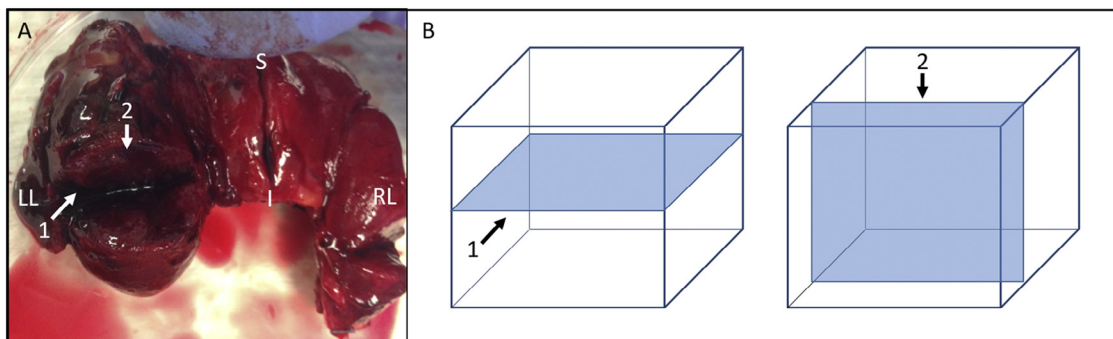

Fig 3. Histology and OCT imaging planes demonstrated on an excised thyroid with papillary carcinoma. (**A**) Thyroid tissue with three surgical incisions on right lobe, left lobe, and isthmus, respectively. (**B**) Schematic wire-frame block representing thyroid tissue along with the (1) OCT imaging plane and (2) orthogonal histologic section plane. OCT, optical coherence tomography; LL, Left Lobe; RL, Right Lobe; S, Superior; I, Inferior. (For interpretation of the references to color in this figure legend, the reader is referred to the Web version of this article.)

Table I. Summary of thyroid cases for tissues imaged ex vivo using the benchtop optical coherence tomography system

Gender	Age	Demographic	Preop diagnosis	Procedure	Final postop diagnosis
F	—	—	Suspicious thyroid nodule	Total thyroidectomy	Follicular adenoma
F	65	White, non-Hispanic	Suspicious thyroid nodule	Total thyroidectomy	Follicular neoplasm
F	—	—	Suspicious thyroid nodule	Total thyroidectomy	Nodular goiter
M	42	—	Suspicious left thyroid nodule	Total thyroidectomy	Papillary microcarcinoma, follicular adenoma, and multinodular goiter
F	35	White, non-Hispanic	Multinodal goiter	Completion thyroidectomy	Multinodular colloid goiter
F	—	—	Suspicious thyroid nodule	Total thyroidectomy	Multinodal goiter
F	24	—	Papillary thyroid carcinoma	Total thyroidectomy with right central neck dissection	Papillary thyroid carcinoma, 12 of 16 positive nodes
F		White, non-Hispanic	Suspicious thyroid nodule	Total thyroidectomy	Colloid goiter with focal adenomatous nodules
F	31	White, non-Hispanic	Graves disease	Total thyroidectomy	Papillary thyroid microcarcinoma, 2 benign parathyroid glands (1 intrathyroidal)
F	74	White, non-Hispanic	Suspicious thyroid nodule	Completion thyroidectomy	multinodular thyroid with adenomatous nodules, and focal Hurthle cell adenomatous nodule (left lobe)
F	64	White, non-Hispanic	Papillary microcarcinoma	Completion thyroidectomy	Multinodular goiter and focal changes (papillary microcarcinoma).
F	—	—	Suspicious thyroid nodule	Total thyroidectomy	Benign thyroid with diffuse hyperplasia
M	71	White, non-Hispanic	Papillary carcinoma, right lobe	Total thyroidectomy	Multinodular colloid goiter with Hurthle cell changes and lymphoid
F	66	—	Multinodal goiter	Total thyroidectomy	Multinodular colloid goiter with postbiopsy site changes
F	—	—	Suspicious thyroid nodule	Total thyroidectomy	Papillary microcarcinoma and multinodular goiter
F	—	White, non-Hispanic	Suspicious thyroid nodule	Total thyroidectomy	Goiter with hyperplastic changes, focal chronic inflammation, and focal entrapped parathyroid tissue; no malignancy is seen.
F	21	White, non-Hispanic	Suspicious thyroid nodule	Total thyroidectomy	Benign thyroid with diffuse hyperplasia and goiter
F	28	White, non-Hispanic	Left thyroid nodule	Left hemithyroidectomy	Nodular goiter with foci of chronic inflammation
F	65	Non-Hispanic, African-American	Toxic multinodular goiter	Total thyroidectomy	Toxic multinodular goiter
F	56	White, non-Hispanic	Toxic multinodular goiter	Total thyroidectomy	Multinodular goiter with adenomatous follicular hyperplasia
F	66	—	Multinodal goiter	Total thyroidectomy	Multinodular colloid goiter with dystrophic calcifications
F	50	—	Papillary thyroid carcinoma	Total thyroidectomy	Papillary carcinoma

Table I. (*continued*)

Gender	Age	Demographic	Preop diagnosis	Procedure	Final postop diagnosis
F		White, non-Hispanic	Suspicious thyroid nodule	Total thyroidectomy	Papillary carcinoma Multiple benign colloid nodules and focal adenomatous hyperplasia
F	26	—	Suspicious thyroid nodule	Total thyroidectomy	Follicular carcinoma Colloid goiter with adenomatous nodule
F	69	—	Hurthle cell neoplasm	Total thyroidectomy.	Left thyroid nodule suspicious for Hurthle cell neoplasm
F	81	—	Suspicious thyroid nodule	Total thyroidectomy	Papillary carcinoma and Hashimoto thyroiditis
F	46	—	Papillary thyroid carcinoma	Total thyroidectomy, limited central neck dissection	Papillary carcinoma, follicular variant, 0 of 6 lymph nodes
F	—	—	Multinodular goiter or follicular neoplasm	Total thyroidectomy	Multiple follicular nodules; outside consultation pending

Abbreviations: *F,* female; *M,* male.

histology and OCT were due to the loss of portions of tissue that occurred during sectioning of histology (performed in house by researchers). The upper panel in Fig 4 shows images from a patient with both regions of goiter and normal thyroid. The OCT image in Fig 4, B, shows rounded outlines of thyroid follicles with relatively uniform size and distribution, whereas the region containing goiter (Fig 4, E) shows regions of higher tissue density and inhomogeneous scattering, large differences in the size of the follicles, and deformation of the tissue structure. Videos of the 3D OCT data set as the imaging plane passes through the normal and goiter regions of the thyroid tissue are shown in the supplementary data (Supplementary Videos S1 and S2). The corresponding histology images are shown in Fig 4, *C and F*, respectively. In the lower panel in Fig 4 are images of normal (Fig 4, H) and diseased (Fig 4, K) thyroid regions from a patient with follicular adenoma and the corresponding histology images (Fig 4, *I* and *L*, respectively). The image of the follicular adenoma exhibits enlarged follicles, denser tissue, and higher scattering compared with the image of the normal region.

The representative OCT image of papillary thyroid carcinoma (Fig 5, E) shows increased scattering and the formation of a tumor capsule, compared with normal thyroid tissue (Fig 5, B). Videos of the OCT image data as the imaging plane passes through the normal and papillary carcinoma regions of the thyroid tissue are shown in the supplementary data (Supplementary Videos S3 and S4). In a case where papillary thyroid carcinoma was combined with Hashimoto thyroiditis (HT), there was no normal tissue found in the thyroid because all the tissues surrounding the cancer contained HT (Fig 5, K). HT is an autoimmune thyroid disease that leads to hypothyroidism. Although the presence of HT alone does not warrant surgery, the association with papillary thyroid carcinoma does require surgical removal, although the correlation between these 2 thyroid pathologies is not entirely understood.[26]

These imaging results using the benchtop system revealed OCT images with different features of normal, benign, and malignant human thyroid tissues. The high percentage of total thyroidectomies that result in benign outcomes upon final histopathology demonstrates the limitation of current diagnostic methods (ie, ultrasound and FNAB). Improvements in imaging technology, particularly during surgical procedures, have the potential to improve patient outcomes by reducing unnecessary thyroidectomies and enabling visualization of cancer metastasis to lymph nodes and other regions of the neck.

Intraoperative imaging of human thyroid tissue. Thyroid specimens from 6 patients (3 males and 3 females, ages 43–61) who were undergoing total thyroidectomy (5 patients) and right hemithyroidectomy (1 patient) were imaged in the operating room using the handheld probe immediately after surgical resection. One thyroid specimen could not be imaged because of the frail cystic nature of the nodular tissue, which ruptured when the surgeon attempted to expose the inner tissue for OCT imaging. The specimen did not contain tangible tissue inside the walls of the cystic thyroid nodule. Table II provides a summary of the human subject cases, including the procedure, the final postoperative diagnosis, and the nodule dimensions and location (if applicable). The final
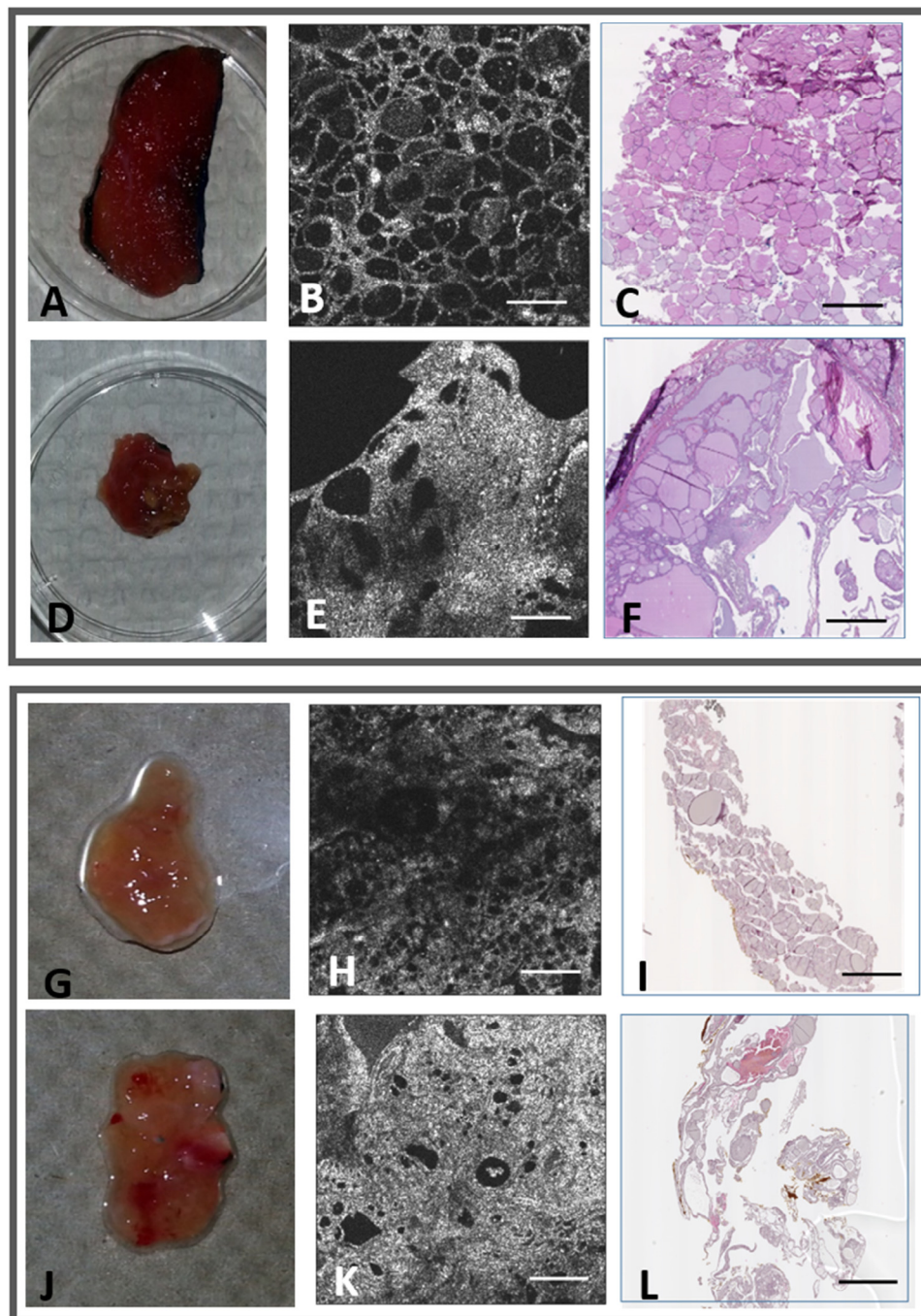
Fig 4. OCT and corresponding histology of normal and benign thyroid tissues. Upper panel: (**A, D**) Photos and (**B, E**) OCT images of normal and goiter tissue regions from the same patient, along with (**C, F**) the corresponding histology images, respectively. Lower panel: (**G, J**) Photos and (**H, K**) OCT images of normal and follicular adenoma tissue regions from the same patient, along with (**I, L**) the corresponding histology images, respectively. All scale bars: 1 mm. OCT, optical coherence tomography.

histopathologic diagnoses included papillary carcinoma, multinodular goiter, and hyperthyroidism.

Representative OCT images of thyroid specimens using our portable intraoperative OCT imaging system are shown in Figs 6 and 7. It should be noted that the images from the intraoperative system are cross-sectional and depth resolved, whereas the images from the benchtop system are en face or acquired in a plane parallel to the tissue surface. The benchtop system was configured on a vibration-isolation optical table and housed in the
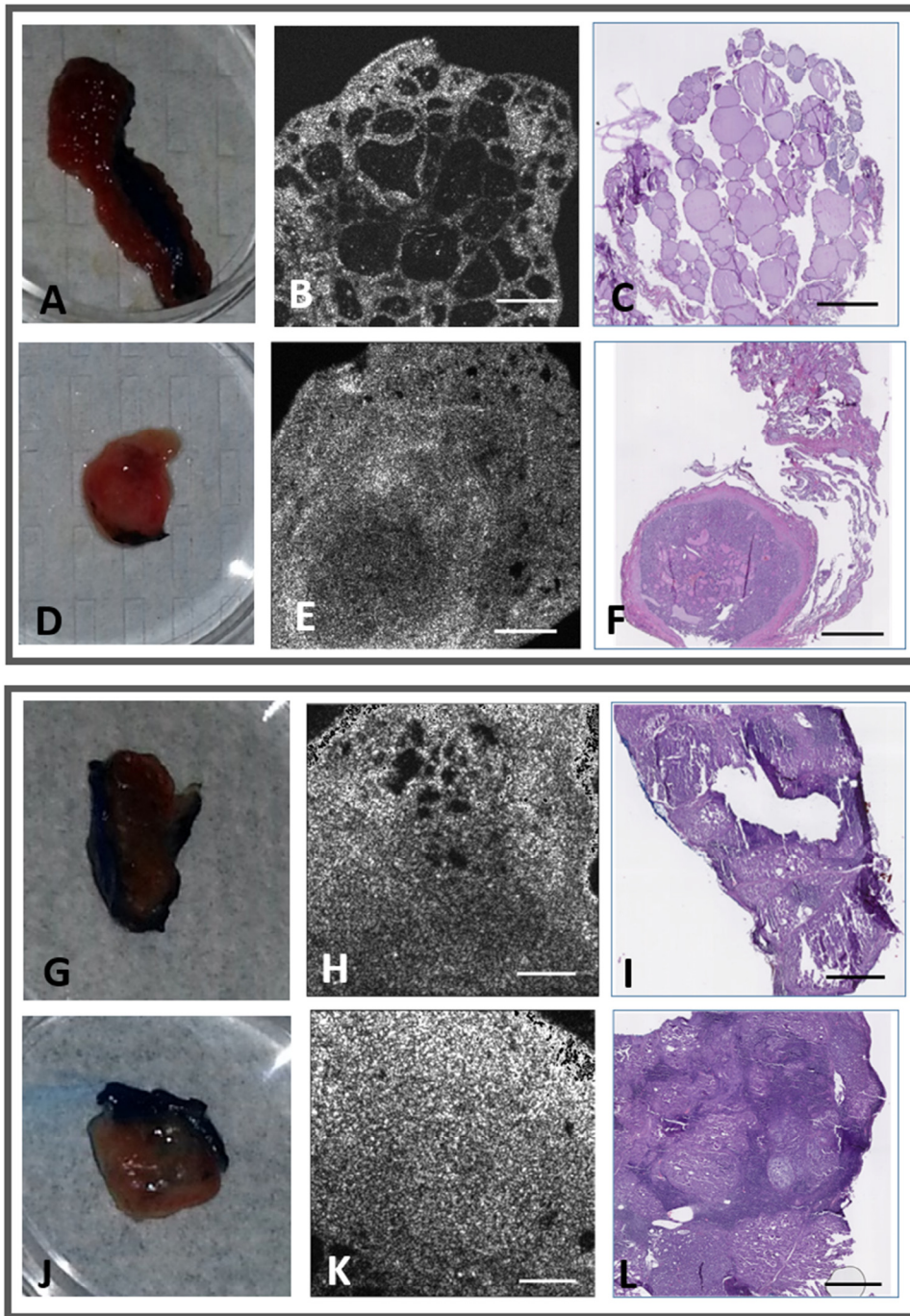
Fig 5. OCT and corresponding histology of normal and papillary thyroid carcinoma tissues. Upper panel: (**A, D**) Photos and (**B, E**) OCT images of normal and papillary thyroid carcinoma tissue regions from the same patient, along with (**C, F**) the corresponding histology images, respectively. Lower panel: (**G, J**) Photos and (**H, K**) OCT images of Hashimoto thyroiditis and papillary thyroid carcinoma tissue regions from the same patient, along with (**I, L**) the corresponding histology images, respectively. All scale bars: 1 mm. OCT, optical coherence tomography.

Table II. Summary of thyroid cases imaged using the intraoperative optical coherence tomography system

Gender	Age	Procedure	Final postop diagnosis	Nodule dimension	Nodule location	Other tissue
F	57	Total thyroidectomy	Multinodular goiter	3.0 mm largest dimension	Right lobe	Normal left lobe
M	53	Total thyroidectomy	Hyperthyroidism and nodule	$(3.1 \times 2.0 \times 1.7)$ cm	Right lobe	Normal left lobe
F	43	Total thyroidectomy	Papillary carcinoma	$(5.0 \times 4.5 \times 4.0)$ cm	Left and right lobe	N/A
F	59	Total thyroidectomy	Papillary carcinoma	$(0.9 \times 0.8 \times 0.7)$ cm	Isthmus	Normal left and right lobe
M	59	Total thyroidectomy	Toxic multinodular goiter	2.5 cm largest dimension	Left lobe	N/A
M	61	Right hemithyroidectomy	Adenomatous nodule	N/A	N/A	Parenchymal

Abbreviations: *F*, female; *M*, male; *N/A*, not applicable.

laboratory, whereas the portable, self-contained intraoperative system was transported to and into the operating room where it was calibrated and tested after the patient was sedated, and before imaging. The benchtop system utilized a stationary sample arm that collects a single 3D OCT image volume, whereas the portable system has a handheld probe that can be swept along the tissue to generate video-based cross-sectional images in real time. For the current study, some of the intraoperative thyroid specimens that were imaged were of comparable size to the probe tip, which did not allow for good video-based image sweeps. For these cases, single sectional images are shown. Furthermore, the intraoperative tissue specimens were not flat, and the OCT operator was not allowed to physically alter the tissue in any way to accommodate for imaging. The tissue also had to be imaged quickly, approximately 5 seconds per area, because it was not placed in a preserving solution before OCT imaging. Two OCT operators were required per imaging session, where the first OCT operator would hold the handheld probe and specimen while the second operator would control

the image acquisition, record the specimen orientation, and digitally photograph the specimen.

Fig 6 shows representative intraoperative OCT images, corresponding histology, and a photo of the gross thyroid tissue from a patient with papillary carcinoma. The OCT images reveal dense, highly scattering tissue and an absence of any normal follicular structure. Fig 6, B, clearly shows a margin between normal and cancerous tissues. The right side of the image shows normal follicular structures with the transition to papillary carcinoma toward the left, where the follicular structures are overcome by dense, highly scattering tissue. Fig 7 shows a representative intraoperative OCT image, corresponding histology, and photo of the gross thyroid tissue from a patient with toxic multinodular goiter. In the OCT image, the follicles appear enlarged and are separated from each other with an overall nonuniform structure.

These images demonstrated real-time imaging of thyroid tissues during surgical procedures. The images were collected using a handheld probe that is capable of imaging in vivo for real-time surgical guidance in future
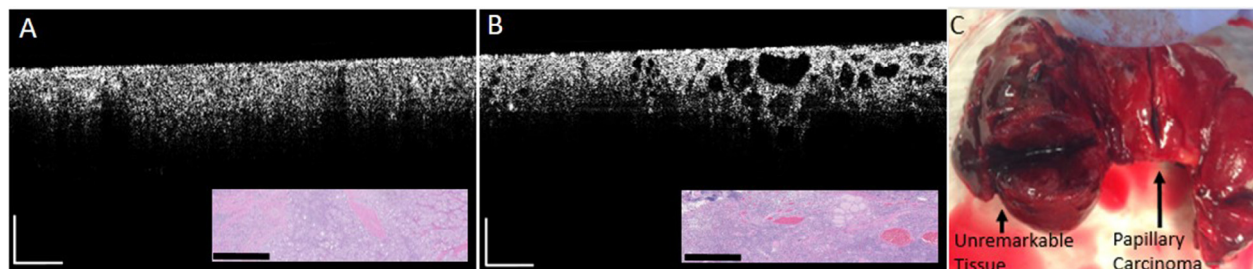

Fig 6. Intraoperative OCT images, corresponding histology, and a photo of the gross thyroid tissue from a patient with papillary carcinoma. (**A**) OCT image of papillary carcinoma with corresponding histology (inset). (**B**) OCT image of a margin that transitions from papillary carcinoma (left) to normal thyroid tissue (right) with corresponding histology (inset). (**C**) Total thyroidectomy specimen showing unremarkable left and right lobes, as well as the isthmus with the localized papillary thyroid carcinoma. Scale bars represent 0.5 cm. OCT, optical coherence tomography.
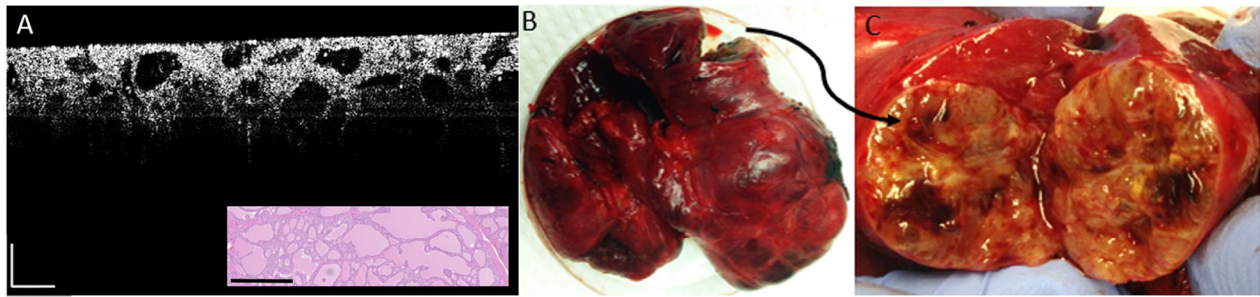
Fig 7. Intraoperative OCT image, corresponding histology, and photo of the gross thyroid tissue from a patient with toxic multinodular goiter. (**A**) OCT image with corresponding histology (inset). (**B**) Total thyroidectomy tissue confined in a Petri dish. (**C**) Photo of exposed tissue following surgical incision of the left lobe of thyroid tissue. Scale bars represent 0.5 cm.

thyroid surgeries, as has been previously demonstrated during wide local excision of breast cancer.[21] OCT imaging with our handheld probe can provide real-time feedback during the procedure rather than waiting for postoperative histopathologic diagnosis, with the overall goal to improve patient morbidity.

DISCUSSION

The present study demonstrated the ability to differentiate normal, benign, and malignant thyroid tissues from the bench to the bedside (operating room). A benchtop OCT system was used to image fresh excised thyroid tissues from 28 patients to establish an atlas of different thyroid diseases and what types of features would be expected during intraoperative imaging. A portable OCT system was subsequently developed to translate the technology to the operating room and used to perform a feasibility study to demonstrate the ability to distinguish normal from benign and malignant tissues in 6 thyroid surgeries, showing the potential of the system for surgical guidance. Real-time OCT imaging during thyroid surgeries could potentially reduce the morbidity associated with total thyroidectomies by enabling surgeons to remove only the diseased portions of the thyroid. This technique would greatly improve patient lives because more than 50% of cases where total thyroidectomy has been performed because of a suspicious nodule are found to be benign upon final histopathology analysis. Current imaging methods used for thyroid diagnostics (eg, ultrasound and FNAB) do not provide real-time feedback during thyroid surgeries. Other groups have also demonstrated OCT of the human thyroid and the capability of this technology for differentiating cancerous and noncancerous thyroid tissues. Our system has the further capability of performing in vivo imaging of the tissue before surgical excision, as well as imaging of the cavity to detect the presence of any remaining cancer. This has been demonstrated during wide local excision surgery

of the breast, and future work will demonstrate in vivo imaging during thyroid surgeries.

There are many challenges encountered when translating a new imaging technology from the bench to clinical use. For these current studies, the instrumentation and optical components of a benchtop OCT system were minimized to fit onto a portable cart that could be easily maneuvered into the operating room. The benchtop system was used initially to identify and establish basic microstructural tissue features that would likely be encountered when using the intraoperative system, and was used initially because it was more robust than the portable handheld system, being more stationary, mounted on an optical table, and located in an isolated laboratory setting. It should be noted that some imaging quality and system performance can be reduced by the nature of the imaging system being transported around the hospital, as opposed to being secured to a stable optical table in the laboratory. The diagnostic performance of the intraoperative system was demonstrated in a previous study using the intraoperative system to image breast tumor margins, which yielded a sensitivity and a specificity of 91.7% and 92.1%, respectively.[21] Ongoing studies to image additional thyroid cases intraoperatively are being performed, and the standard sensitivity-and-specificity analysis will be performed based on diagnoses by clinicians trained on reading the OCT images. Additionally, a foot pedal can be incorporated into the system so that a single user can initiate and stop the recording of data, thus minimizing the number of people in the operating room.

Another challenge during intraoperative imaging was the restriction that the OCT imaging plane be orthogonal to the histologic sectioning plane. This restriction prevented direct correlation and precise feature matching between the OCT and histology images for the intraoperative cases, whereas with the benchtop system, the excised tissues could be inked after imaging, and the histology planes could be clearly matched by the study

investigators. This allowed a more direct correlation between OCT and histology. Future studies will be performed where multiple tissue samples will be imaged with the portable OCT system in the pathology laboratory to achieve more direct histologic comparisons and to assess the diagnostic accuracy of the system. Additionally, imaging the thyroid intraoperatively (and potentially in vivo in future studies) is restricted to the exposed surface and near-surface regions of the tissue, because OCT has an imaging depth of 1–2 mm. For the cases presented here, the surgeon made an incision in the thyroid to allow for direct imaging of the area of interest. For future in vivo studies, the surgical protocol would be modified such that once the thyroid is exposed but still in place during the surgery, the surgeon would use the probe to image regions of interest to further indicate the presence and extent of cancer. The imaging feedback occurs in real time at a near-video rate and would require additional time on the order of about 5–10 minutes, depending on the surgeon and the case. The immediate anticipated clinical impact would be for patients who are recommended to undergo total thyroidectomy for a suspicious nodule. For these cases, our system could be used to better explore the thyroid in situ during the open surgery, and the surgeon could modify the procedure to a hemithyroidectomy or lobectomy where appropriate to improve patient morbidity.

The implementation of OCT needle probes with the portable intraoperative system could be used to image and identify tissue microstructure in deeper regions of the thyroid.[27,28] In future studies, the portable system presented here could also be used to perform in vivo imaging of the surgical cavity and any exposed locoregional lymph nodes with the handheld probe, immediately after removal of the primary specimen. This system and method has been previously demonstrated for breast cancer surgery.[21] This intraoperative in vivo imaging system would enable immediate visualization of any residual tumor tissue during surgery, as well as evidence of any disease in other regions of the neck and lymph nodes.[29]

CONCLUSION

This feasibility study demonstrated the translation of OCT imaging of the human thyroid from the bench to the operating room using a portable intraoperative system with a handheld surgical imaging probe. Further improvements to the technology would enable the surgeon to assess the in vivo thyroid, including deep thyroid nodules, in real time during surgery, and possibly to reduce the number of unnecessary total thyroidectomies because of suspicious diagnoses.

Supplementary Data

Supplementary data related to this article can be found, in the online version, at doi:10.1016/j.trsl.2017.12.001.

REFERENCES

1. Howlader N, Noone AM, Krapcho M, Miller D, Bishop K, Kosary CL, Yu M, Ruhl J, Tatalovich Z, Mariotto A, Lewis DR, Chen HS, Feuer EJ, Cronin KA, eds. SEER Cancer Statistics Review, 1975-2014. Bethesda, MD: National Cancer Institute.Available at: https://seer.cancer.gov/csr/1975_2014/. Accessed December 25, 2017.
2. Terris DJ, Gourin CG, eds. Thyroid and parathyroid diseases: medical and surgical management. New York, NY: Thieme Medical Publishers, Inc.; 2009.
3. Niedziela M. Thyroid nodules. Best Pract Res Clin Endocrinol Metab 2014;28:245–77. doi:10.1016/j.beem.2013.08.007.
4. Chaudhary V, Bano S. Imaging of the thyroid: recent advances. Indian J Endocrinol Metab 2012;16:371–6. doi:10.4103/2230-8210.95674.
5. Castro MR, Gharib H. Continuing controversies in the management of thyroid nodules. Ann Intern Med 2005;142:926–31.
6. Alexander EK. Approach to the patient with a cytologically indeterminate thyroid nodule. J Clin Endocrinol Metab 2008;93:4175–82. doi:10.1210/jc.2008-1328.
7. Dobrinja C, Trevisan G, Piscopello L, Fava M, Liguori G. Comparison between thyroidectomy and hemithyroidectomy in

treatment of single thyroid nodules identified as indeterminate follicular lesions by fine-needle aspiration cytology. Ann Ital Chir 2010;81:403–10.

8. Gibelli B, Dionisio R, Ansarin M. Role of hemithyroidectomy in differentiated thyroid cancer. Curr Opin Otolaryngol Head Neck Surg 2015;23:99–106. doi:10.1097/MOO.0000000000000142.

9. Huang D, Swanson EA, Lin CP, et al. Optical coherence tomography. Science 1991;254:1178–81.

10. Baumal CR. Clinical applications of optical coherence tomography. Curr Opin Ophthalmol 1999;10:182–8.

11. Das A, Sivak MV Jr, Chak A, et al. High-resolution endoscopic imaging of the GI tract: a comparative study of optical coherence tomography versus high-frequency catheter probe EUS. Gastrointest Endosc 2001;54:219–24.

12. Tsai TH, Fujimoto JG, Mashimo H. Endoscopic optical coherence tomography for clinical gastroenterology. Diagnostics (Basel) 2014;4:57–93. doi:10.3390/diagnostics4020057.

13. Cao T, Tey HL. High-definition optical coherence tomography—an aid to clinical practice and research in dermatology. J Dtsch Dermatol Ges 2015;13:886–90. doi:10.1111/ddg.12768.

14. Gambichler T, Jaedicke V, Terras S. Optical coherence tomography in dermatology: technical and clinical aspects. Arch Dermatol Res 2011;303:457–73. doi:10.1007/s00403-011-1152-x.

15. Cruz Ferreira R, Pereira-da-Silva T, Patrício L, Bezerra H, Costa M. Coronary optical coherence tomography: a practical overview of current clinical applications. Rev Port Cardiol 2016;35:105–12. doi:10.1016/j.repc.2015.09.016.

16. Yonetsu T, Bouma BE, Kato K, Fujimoto JG, Jang IK. Optical coherence tomography—15 years in cardiology. Circ J 2013;77:1933–40.

17. Shelton RL, Jung W, Sayegh SI, McCormick DT, Kim J, Boppart SA. Optical coherence tomography for advanced screening in the primary care office. J Biophotonics 2014;7:525–33. doi:10.1002/jbio.201200243.

18. Nguyen FT, Zysk AM, Chaney EJ, et al. Intraoperative evaluation of breast tumor margins with optical coherence tomography. Cancer Res 2009;69:8790–6. doi:10.1158/0008-5472.CAN-08-4340.

19. Allen WM, Chin L, Wijesinghe P, et al. Wide-field optical coherence micro-elastography for intraoperative assessment of human breast cancer margins. Biomed Opt Express 2016;7:4139–53.

20. Mesa KJ, Selmic LE, Pande P, et al. Intraoperative optical coherence tomography for soft tissue sarcoma differentiation and margin identification. Lasers Surg Med 2017;49:240–8. doi:10.1002/lsm.22633.

21. Erickson-Bhatt SJ, Nolan RM, Shemonski ND, et al. Real-time imaging of the resection bed using a handheld probe to reduce incidence of microscopic positive margins in cancer surgery. Cancer Res 2015;75:3706–12. doi:10.1158/0008-5472.CAN-15-0464.

22. Pantanowitz L, Hsiung PL, Ko TH, et al. High-resolution imaging of the thyroid gland using optical coherence tomography. Head Neck 2004;26:425–34.

23. Zhou C, Wang Y, Aguirre AD, et al. *Ex vivo* imaging of human thyroid pathology using integrated optical coherence tomography and optical coherence microscopy. J Biomed Opt 2010;15:016001. doi:10.1117/1.3306696.

24. Ladurner R, Hallfeldt KK, Al Arabi N, Stepp H, Mueller S, Gallwas JK. Optical coherence tomography as a method to identify parathyroid glands. Lasers Surg Med 2013;45:654–9. doi:10.1002/lsm.22195.

25. Sommerey S, Al Arabi N, Ladurner R, et al. Intraoperative optical coherence tomography imaging to identify parathyroid glands. Surg Endosc 2015;29:2698–704. doi:10.1007/s00464-014-3992-x.

26. Anand A, Singh KR, Kushwaha JK, Hussain N, Sonkar AA. Papillary thyroid cancer and Hashimoto's thyroiditis: an association less understood. Indian J Surg Oncol 2014;5:199–204. doi:10.1007/s13193-014-0325-4.

27. Lorenser D, Yang X, Kirk RW, Quirk BC, McLaughlin RA, Sampson DD. Ultrathin side-viewing needle probe for optical coherence tomography. Opt Lett 2011;36:3894–6. doi:10.1364/OL.36.003894.

28. Zysk AM, Nguyen FT, Chaney EJ, et al. Clinical feasibility of microscopically-guided breast needle biopsy using a fiber-optic probe with computer-aided detection. Technol Cancer Res Treat 2009;8:315–21.

29. Nolan RM, Adie SG, Marjanovic M, et al. Intraoperative optical coherence tomography for assessing human lymph nodes for metastatic cancer. BMC Cancer 2016;16:144. doi:10.1186/s12885-016-2194-4.